Quantification of the Long-Term Performance of Steels T91 and 316L in Oxygen-Containing Flowing Lead-Bismuth Eutectic at 550°C

Carsten Schroer

Juergen Konys

Institut fuer Materialforschung III,
Karlsruher Institut fuer Technologie (KIT),
Hermann-von-Helmholtz-Platz 1,
76344 Eggenstein-Leopoldshafen, Germany

The long-term performance of ferritic/martensitic steel T91 and austenitic 316L in oxygen-containing flowing lead-bismuth eutectic at 550°C was investigated by exposing the materials for up to 15,000 h in the CORRIDA loop. The velocity of the liquid-metal flow was 2 m/s and the concentration of dissolved oxygen averaged 1.6×10^{-6} mass %. The resulting corrosion processes and products were analyzed and quantified using metallographic methods. [DOI: 10.1115/1.4000364]

1 Introduction

Depending on the function fulfilled in the plant, plant components may experience various loads, which, in general, are thermal, mechanical, and/or chemical (corrosive) in nature. In nuclear plants, some of the components are additionally exposed to radiation. Most materials, especially steels, which are often favored because of the widely available operational data as well as for economic reasons, degrade under the prevailing conditions, so that the lifetime of plant components is generally limited. For an adequate material selection, proper design of components, and safe operation, the decisive degradation mechanisms must be identified and their impact on material properties quantified.

When heavy liquid metals (HLMs) such as liquid lead (Pb) or lead-bismuth eutectic (LBE) are used as the process medium, corrosion can be the lifetime-determining factor for the plant components. As these liquid metals are designed as primary coolants in nuclear plants, not only the influence of corrosion on structural integrity but also the impact on heat transfer is of importance. The latter is especially true for the cladding of the fuel rods and parts of the heat-exchanger system, which are affected by high thermal loads under service conditions.

In the framework of the European integrated project (IP) EUROTRANS (Contract No. FI6W-CT-2004-516520), the long-term performance of the ferritic/martensitic (F/M) steel T91 and austenitic stainless-steel 316L at 550°C in flowing LBE was investigated, primarily to broaden the database for a quantitative assessment of the component lifetime in future European demonstration plants for the transmutation of nuclear waste in an accelerator driven system (ADS). As the formation of an oxide scale on the surface of the steels can prevent or at least minimize crucial phenomena such as the dissolution of steel constituents and embrittlement induced by the liquid metal, oxygen was added to the LBE, targeting 10^{-6} mass % dissolved oxygen. Specimens of the steels were exposed to the liquid metal for up to 15,000 h and examined with respect to the loss of sound material and the structure and thickness of the oxide scales formed using metallographic methods. The knowledge of the thickness (and composition of distinguishable parts) of the oxide scales not only allows quantifying the expected degradation of heat-transfer properties but also, in combination with the material loss, estimating the amount of steel constituents dissolved in the liquid metal, which is important for mass transfer from hot to cold regions, i.e., the potential for plugging along the liquid-metal flow path.

2 Experimental

2.1 Sample Materials and Specimen Preparation. The materials investigated in this study are the F/M steel T91 (ASTM A387 Grade 91 Cl2) with nominally 7.90–9.60 mass % chromium (Cr) and 0.80–1.10 mass % molybdenum (Mo), and the austenitic steel 316L (ASTM A240 316L) nominally containing 16.00–18.00 mass % Cr, 2.00–3.00 mass % Mo, and 10.00–14.00 mass % nickel (Ni). These steels were delivered in the form of hot-rolled and heat-treated 15 mm thick plates [1]. Details on the final heat treatment and actual chemical composition of the steels are given in Table 1. The microstructure consists of tempered martensite and austenite for T91 and 316L, respectively. The majority of precipitates observed in the martensitic structure of T91 are of the type $M_{23}C_6$, but M_6C carbides are also found at grain boundaries and comparatively small coherent carbonitrides are present inside the martensite laths [1]. Inclusions of secondary phases identified in the austenitic structure of 316L are manganese (Mn) sulfide or complex oxides (slag).

The specimens for the exposure to flowing oxygen-containing LBE (performed in the CORRIDA loop at the liquid-metal laboratory of the Forschungszentrum Karlsruhe) are cylinders with dimensions $\varnothing 8\times 35$ mm^2 that have an internal and an external screw thread, so as to combine a number of specimens for simultaneous exposure. These specimens were mechanically machined and finished by turning, resulting in a maximum peak-to-valley height of the surface profile in the range 1.5–2 μm. The arithmetic and geometric mean deviations of the surface profile from the centerline are 0.20 μm and 0.25 μm, respectively. Prior to exposure, the actual diameter in the center and near both ends was measured for each specimen with an accuracy of 2–4 μm as a basis for the metallographic quantification of the corrosion damage [2]. Finally, the surface of the specimens was cleaned with acetone.

2.2 Testing Conditions. Specimens of T91 and 316L were exposed to flowing oxygen-containing LBE in the CORRIDA loop [3] for nominally 500 h, 1000 h, 2000 h, 4000 h, 7500 h, 10,000 h, and 15,000 h. For each material and exposure time, two specimens were employed, one of which was chosen for metallo-

Contributed by the International Gas Turbine Institute of ASME for publication in the JOURNAL OF ENGINEERING FOR GAS TURBINES AND POWER. Manuscript received July 22, 2009; final manuscript received August 5, 2009; published online May 27, 2010. Editor: Dilip R. Ballal.

Table 1 Chemical composition in mass % and final heat-treatment of the investigated steels [1]

T91													
Fe	Cr	Mo	Mn	Si	V	Ni	Nb	Cu	Al	C	N	P	S
Bal.	8.99	0.89	0.38	0.22	0.21	0.11	0.06	0.06	0.0146	0.1025	0.0442	0.021	0.0004
Heat treatment: Normalizing at 1050°C (1 min/mm thickness) and tempering at 770°C (3 min/mm)													

316L													
Fe	Cr	Ni	Mo	Mn	Si	Cu	V	W	Al	C	N	P	S
Bal.	16.73	9.97	2.05	1.81	0.67	0.23	0.07	0.02	0.0183	0.0185	0.0293	0.032	0.0035
Heat treatment: solution annealing at 1050–1100°C													

graphic post-test analysis after visual inspection; the second specimen of the same material and exposure time was additionally examined if the first gave ambiguous results. Except for short periods during which conditions stabilized after exchanging specimens, the temperature, T, and the velocity of the liquid-metal flow, v, in the test sections of the loop (where the specimens resided) were $T=550(+5)°C$ and $v=2.0(\pm 0.2)$ m/s. The oxygen content of the LBE was measured over the entire runtime of the exposure experiment using an electrochemical oxygen sensor with a platinum (Pt)/air reference electrode that resides at the inlet of the (in direction of the liquid-metal flow) first test section. The sensor output, E, and the calculated oxygen concentration, c_O, which follows as [4]

$$\log(c_O/\text{mass }\%) = -3.2837 + \frac{6949.8}{T/K} - 10080\frac{E/V}{T/K} \qquad (1)$$

are depicted as a function of the runtime of the experiment in Fig. 1. Additionally, the oxygen concentrations necessary for the formation of magnetite (Fe_3O_4) and Ni oxide (NiO) from the pure metals are indicated in this figure, showing that Fe_3O_4 and, consequently, also the more stable Fe–Cr spinel ($FeCr_2O_4$) and chromia (Cr_2O_3) could always form; oxidation of Ni was possible only during short periods in which c_O was about 10^{-5} mass % and higher. On average, the oxygen concentration in the course of the exposures of T91 and 316L was in the range 1.6×10^{-6} mass %. Furthermore, Fig. 1 shows the actual exposure times of the steel specimens and the respective exposure intervals in relation to the runtime of the experiment.

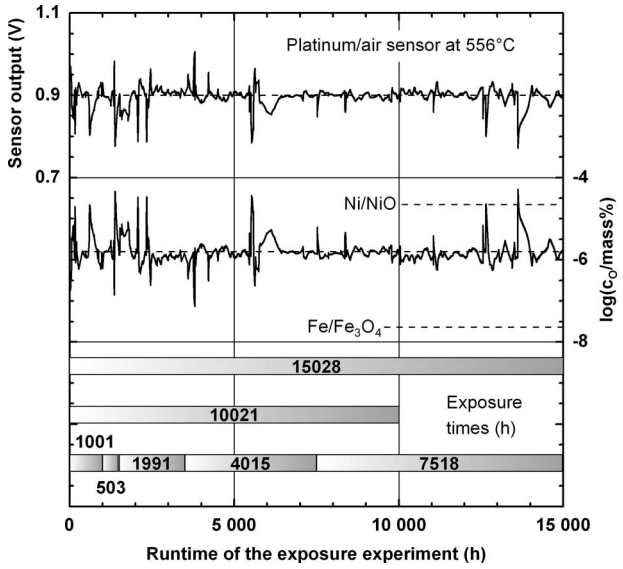

Fig. 1 Parameters of the exposure experiment in flowing oxygen-containing LBE other than temperature (550[+5]°C) and flow velocity (2[±0.2] m/s)

2.3 Post-Test Examinations. After exposure to LBE, two segments were cut from the specimens, one for the preparation of a longitudinal cross section covering a distance of about 10 mm parallel to the direction of the liquid-metal flow during the experiment; the second piece is a circular slice of about 5 mm, which was used for preparing a vertical cross section from approximately the center of the specimen. Most of the post-test examinations were performed on the vertical cross section, including qualitative and quantitative metallographies in the light-optical microscope (LOM) and scanning electron microscope (SEM) supplemented by qualitative energy-dispersive X-ray microanalysis (EDX). The longitudinal cross section was only qualitatively examined in the LOM to check for corrosion phenomena not observed in the central cross section. In the case of the specimens of T91 and 316L, which were exposed for 15,000 h, the analysis of a longitudinal cross section had to be omitted but the respective second specimens were also investigated in vertical cross section.

For each exposure time, the material loss was calculated from the diameter of the specimen core that was not affected by the oxygen-containing LBE—measured in the LOM in six positions uniformly distributed along the vertical cross section [2]—and the initial specimen diameter before the exposure. Additionally, 12 measurements of the thickness of distinguishable parts of the observed corrosion scales—oxide layers adhering to the surface, a zone in the material affected by subsurface corrosion phenomena, etc.—were performed. In the case of most specimens of 316L, the determination of the material loss had to be adapted to pronouncedly nonuniform corrosive attack. As a basis for the prediction of the material loss and scale thickness at times exceeding 15,000 h, the time dependence of the measured quantities was analyzed using mathematical models. (It should be noted that, in the following, material loss is half the loss in diameter of the cylindrical specimens.)

3 Results and Discussion

3.1 T91. Under the conditions of the exposure experiment, steel T91 is capable of forming a continuous oxide scale, generally consisting of an Fe–Cr mixed oxide and an internal oxidation zone (IOZ) between the mixed-oxide layer and the steel (Fig. 2(*a*)). In accordance with the qualitative EDX measurements and recently published results of quantitative electron-probe microanalyses (EPMAs) performed on T91 after oxidation in stagnant LBE at 470°C [5], the mixed oxide is a Cr-deficient spinel ($Fe(Fe_xCr_{1-x})_2O_4$). Inside the IOZ, oxide particles precipitated from the steel matrix after ingress of oxygen along the grain boundaries, dislocations, or other structural defects. These particles consist of oxides more stable than the Cr-deficient spinel forming the oxide layer, i.e., especially of stoichiometric spinel ($FeCr_2O_4$) or Cr_2O_3. The surrounding steel is depleted in Cr, corroborating preferential oxidation of Cr in the IOZ. Cr depletion of the steel beneath the IOZ is, if present, not significant for this type of scale on T91. The volume fraction of oxide in the IOZ was estimated from electron-optical micrographs after exposure for

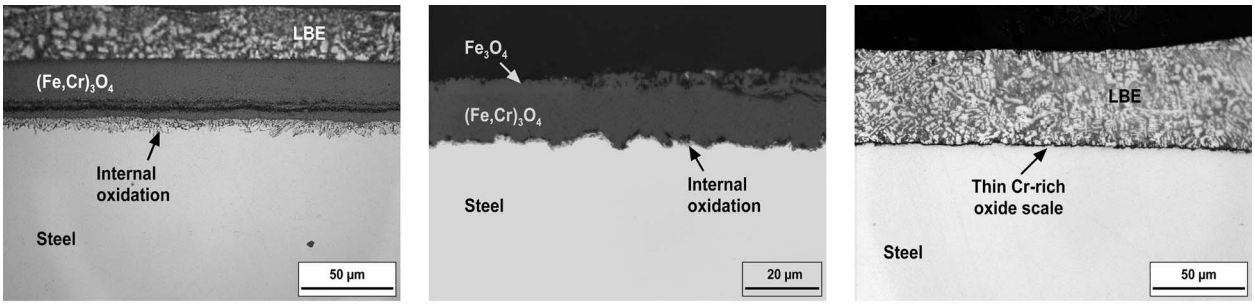

(*a*) (*b*) (*c*)

Fig. 2 Oxide scales on the surface of T91 after exposure for 4015 h (*a*), 503 h (*b*), and 1991 h (*c*) to flowing oxygen-containing LBE at 550°C (v=2 m/s; $c_O \approx 1.6\times10^{-6}$ mass %)

15,028 h as 10–15%. Small amounts of Fe_3O_4 were observed locally on top of the spinel layer, especially after exposure for 503 h (Fig. 2(*b*)). Alternatively, an exceptionally thin scale consisting of a comparatively Cr-rich oxide—$FeCr_2O_4$ or Cr_2O_3—may temporarily establish on the steel surface (Fig. 2(*c*)), but over time apparently merges into the faster-growing scale described above.

The oxide scales depicted in Fig. 2 are obviously efficient barriers between the steel and LBE, so that the liquid metal basically acts as a source of oxygen for the oxidation processes and a sink for steel constituents not completely retained in the oxide scale (e.g., for Fe, as discussed below). However, even after the shortest exposure time in this study, local ingress of liquid metal into the oxide scale was observed, accumulating in the apparently more porous inner part of the spinel layer. Figure 3(*a*) shows an example of the infiltration of the inner part of the spinel layer by Pb and bismuth (Bi), indicating a vertical crack in this layer as the likely path for the ingress of liquid metal. In the absence of cracks, open porosity may provide alternative paths. Especially for exposure times ≤4000 h, an IOZ can be missing where Pb and Bi infiltrated the inner part of the spinel layer; instead, the steel is slightly depleted in Cr at the interface with the spinel. With increasing exposure time, inclusions of solidified liquid metal in the (initially) more compact outer part of the spinel layer occurred more frequently (Fig. 3(*b*)). Except for the specimen exposed for 503 h, Fe_3O_4 formed locally on top of the spinel layer especially where Pb and Bi accumulated inside this layer and, additionally, Cr-rich oxides were occasionally found in the LBE adjacent to the oxide scale surface, indicating that the liquid-metal phase changes the conditions for transport of steel constituents in the scale. At specific sites—possibly, where the amount of Pb and Bi in the inner part of the spinel layer exceeds a certain limit—Cr preferentially dissolves in the liquid-metal phase directly from the steel, resulting in Cr-depleted steel penetrated by liquid metal and a significant local increase in material degradation (Fig. 3(*c*)). The prerequisite for selective leaching of Cr is the depletion of oxygen in the liquid metal inside the oxide scale, as, at low oxygen potentials, Cr exhibits a higher solubility in Pb–Bi alloys than Fe [4]. After diffusion in the liquid-metal phase, Cr reprecipitates at the higher oxygen potentials adjacent to the scale surface, forming Cr-rich oxides as part of a heterogeneous mixture with Fe_3O_4 and the typical spinel. Local selective leaching of Cr occurred especially on specimens with exposure times ≥7500 h, but also specimens exposed for shorter times showed indications of the onset of selective leaching.

The results of quantifying the oxidation of T91 in flowing LBE are summarized in Fig. 4. Figure 4(*a*) shows the material loss in terms of the average recession of the original steel (metal recession) due to the external scale formation, partial dissolution of steel constituents, and internal oxidation as a function of exposure time. Slight Cr depletion was neglected. The corresponding thickness of the spinel layer on the steel surface and thickness of the IOZ are depicted in Fig. 4(*b*). In order to increase the number of data points for characterizing the spinel layer, parts of this layer locally infiltrated by Pb and Bi were included in the calculation of the mean thickness, unless buckling of the scale resulting from liquid-metal infiltration was evident; substantial selective leaching of Cr, as shown in Fig. 3(*c*), was regarded as exceptional behavior and treated separately from "regular oxidation." Both the local metal recession and thickness of the oxide scale formed in the course of regular oxidation became increasingly nonuniform with increasing exposure time. After 7518 h and 15,028 h, thicker parts of the spinel layer contained some Fe_3O_4 (Fig. 5(*b*)), locally accounting for up to 30–35 μm of the layer thickness. In addition to average values and the deviation of the minimum and maximum of, in general, 6 and 12 measurements of the metal recession and thickness of distinguishable parts of the scale, respectively, Fig. 4 shows logarithmic general power functions and/or parabolic rate laws fitted to the experimental data, as a basis for predicting trends at times exceeding 15,000 h. For evaluating parabolic trends, only exposure times ≤4000 h were considered. The thick-

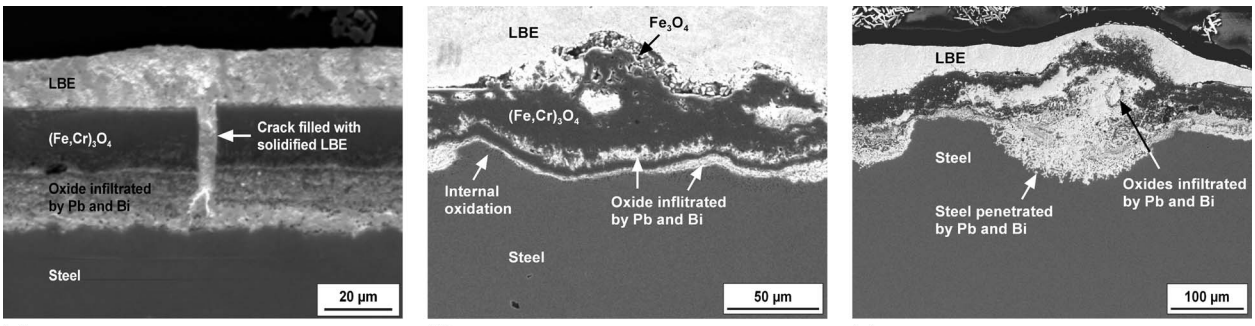

(*a*) (*b*) (*c*)

Fig. 3 Examples of ingress of liquid metal into the oxide scale on T91 after exposure for 4015 h (*a*), 10,012 h (*b*), and 15,028 h (*c*) to flowing oxygen-containing LBE at 550°C (v=2 m/s; $c_O \approx 1.6\times10^{-6}$ mass %)

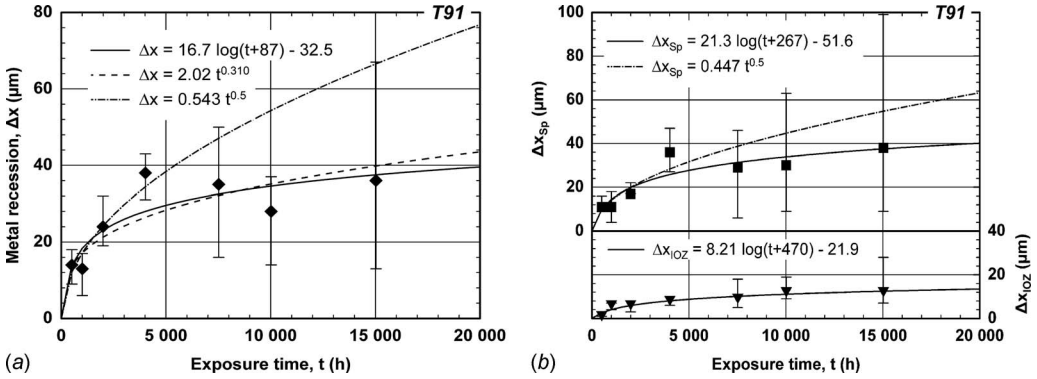

Fig. 4 Material loss (metal recession) and thickness of the spinel layer (Δx_{sp}) and IOZ (Δx_{IOZ}) as a function of time for T91 after exposure to flowing oxygen-containing LBE at 550°C (v=2 m/s; $c_O \approx 1.6\times10^{-6}$ mass %)

ness of Fe_3O_4 occasionally found on top of the spinel layer was either significantly smaller or in the order (only after exposure for 503 h) of the observed variations in the spinel-layer thickness.

In a previously published paper on the performance of T91 in oxygen-containing flowing LBE at 550°C [3], it was discussed that, starting from the nuclei of Me_3O_4-type oxides with various Fe:Cr ratios, Cr-deficient spinel grows toward the core of the steel by inward-diffusion of oxygen, with excess oxygen (not bound in the spinel layer) causing internal oxidation of the steel. If the volume increase due to oxide formation inside the initial bounds of the steel is compensated by outward-diffusion of steel constituents, the surface of the spinel layer coincides with the initial steel surface, which was found by experiments on F/M steel partially surface-alloyed with aluminum (Al) in stagnant liquid Pb [6], and is also corroborated by Fig. 4, indicating a good correspondence between the sum of the spinel and IOZ thickness and the independently determined metal recession, at least for exposure times $\leq$4000 h. For exposure times $\geq$7500 h, the locally measured metal recession was often significantly smaller than the associated sum of spinel and IOZ thickness (possibly resulting from an elliptical distortion of the specimen cross section after preparation for measurements in the LOM [2] concealed by a nonuniform scale thickness along the specimen perimeter), but the correspondence is satisfying when respective averages are regarded. As Cr, once bound to oxygen, is apparently immobile in the inward-growing oxide scale [7], it is mainly Fe diffusion in the spinel layer, which alleviates the volume increase resulting from spinel formation and internal oxidation. In contrast to stagnant conditions, Fe passing through the spinel layer is not predominantly retained as Fe_3O_4 forming on the spinel surface but in large part removed by the liquid-metal flow. At constant c_O, the amount of Fe_3O_4 adhering to the oxide scale decreases with increasing flow velocity of the LBE (1–3 m/s), suggesting erosion of Fe_3O_4 as a mechanism for the removal of Fe from the scale [8]. However, the presence of adherent Fe_3O_4 depends on c_O at constant v (2 m/s) [3], indicating an influence of the Fe solubility (which decreases with increasing c_O according to the solubility product of Fe_3O_4). Therefore, Fe dissolution seems to be more likely than erosion. Porosity in the inner part of the spinel, which is evident especially from Figs. 5(*a*) and 2(*a*), hints that Fe eventually diffuses faster than oxygen, so that, with respect to the volume balance between oxide formation and steel consumption, Fe transport to the spinel surface overcompensates oxide growth at the inner spinel interface. Pb and Bi entering the scale via cracks or open porosity in the outer part of the spinel layer accumulate adjacent to the spinel/steel or spinel/IOZ interface, establishing paths for even faster Fe transport after dissolution in an oxygen-depleted liquid-metal phase, which increases the Fe activity at the spinel-layer surface. The rise in Fe activity favors formation of Fe_3O_4 on top of the spinel and, depending on the (local) magnitude, also Fe_3O_4 formation within the spinel layer, where the expected oxygen activity is smaller than immediately at the surface. An especially crucial situation arises from the ingress of Pb and Bi, if, as discussed above, the oxygen-depleted liquid-metal phase dissolves and, therefore, mobilizes significant amounts of Cr directly from the steel.

Considering the rate laws established from the quantitative data on the oxidation of T91 in flowing LBE (Fig. 4), logarithmic extrapolation of the metal recession predicts a material loss of $\sim$50 μm after 100,000 h at 550°C, v=2 m/s, and $c_O \approx 1.6\times10^{-6}$ mass %. The more conservative estimate from the

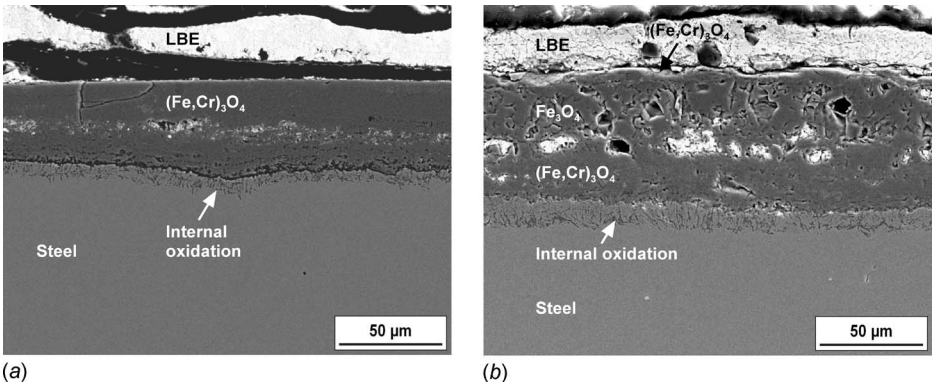

Fig. 5 Oxide scales not significantly affected by ingress of liquid metal on T91 after exposure for 15,028 h to flowing oxygen-containing LBE at 550°C (v=2 m/s; $c_O \approx 1.6\times10^{-6}$ mass %)

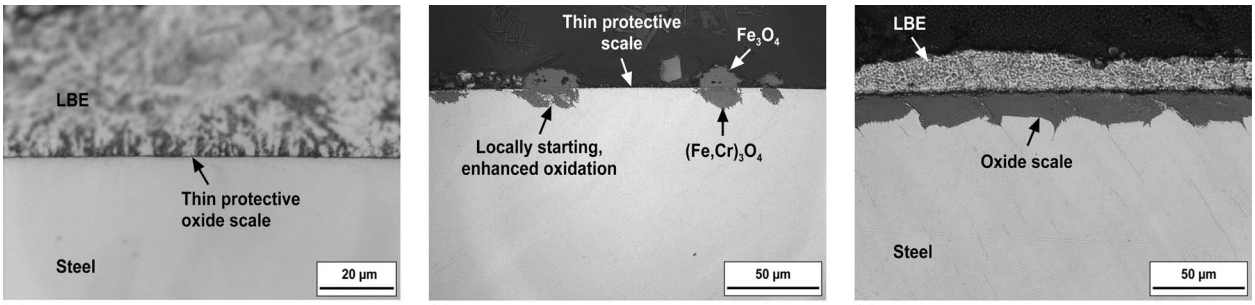

(*a*) (*b*) (*c*)

Fig. 6 Oxide scales on 316L after exposure for 503 (*a*), 4015 (*b*), and 15,028 h (*c*) to flowing oxygen-containing LBE at 550°C (v=2 m/s; $c_O \approx 1.6\times10^{-6}$ mass %)

general power law with exponent 0.31 yields ~70 μm. Using the parabolic trend (exponent 0.5) obtained from data for exposure times ≤4000 h—meeting the maximum values of the metal recession measured for ≥7500 h—yields ~170 μm after 100,000 h, which can be regarded as a worst-case estimate for the regular oxidation of T91. Setting a limit of 100 μm for the material loss on thin-walled components, the minimum service time (according to the parabolic rate law) is ~34,000 h or 4 years; being optimistic, a material loss of 100 μm is not achieved within 20 years. Regarding the thickness of the spinel layer, which potentially reduces the efficiency of heat-transfer surfaces, predictions for 100,000 h are ~55 μm and 141 μm using the logarithmic and parabolic rate laws, respectively, for the spinel thickness, Δx_{sp}, shown in Fig. 4. For estimating the flux of Fe, j_{Fe}, toward the spinel surface, complete retention of Cr in the spinel layer is assumed, so that the change in the partial density of Fe, $\Delta\rho_{Fe}$, for the volume-neutral transformation of T91 into spinel is −4.3 g/cm^3 (at given densities of T91 and spinel of 7.7 g/cm^3 and 4.79 g/cm^3, respectively). Neglecting 10–15 vol % oxides formed in the IOZ, j_{Fe}, results from the rate law for spinel growth as

$$j_{Fe} = \Delta\rho_{Fe}\frac{d}{dt}\Delta x_{sp} \tag{2}$$

Using the parabolic approach, $j_{Fe}<70$ mg/m^2 h after 200 h and <10 mg/m^2 h after 1000 h; $j_{Fe}<20$ mg/m^2 h after 200 h and <1 mg/m^2 h after 1000 h follows from the logarithmic rate law of spinel growth. Under the conditions of the exposure experiment, Fe transported in the spinel layer is predominantly dissolved or, if applicable, eroded after formation of Fe_3O_4 on top of the spinel.

The material loss accompanying locally occurring selective leaching of Cr (after ingress of Pb and Bi into the spinel layer) was measured in the LOM and also using electron-optical micrographs. The maximum loss observed is in the range 150–175 μm after 15,028 h. As selective Cr leaching is probably linked to a critical amount of liquid metal at the spinel/steel interface, the likely trigger for this process are cracks in the spinel layer, as shown in Fig. 3(*a*). However, as long-term experiments in the CORRIDA loop on other F/M steels showed [9], ingress of liquid metal into the spinel layer and selective Cr leaching do not inevitably occur for F/M steels with 9% Cr, but can be prevented, e.g., by optimizing the microstructure with respect to fast Cr diffusion, promoting the formation of Cr-rich oxides at the spinel/steel interface, and, as a result of slower oxide growth, making the scale less prone to defect formation.

3.2 316L. The performance of 316L in flowing oxygen-containing LBE at 550°C, v=2 m/s, and $c_O \approx 1.6\times10^{-6}$ mass % ranges from negligible corrosion (oxidation) with the presence of a thin protective oxide scale on the steel surface (Fig. 6(*a*)) to severe local degradation arising from selective leaching of steel components, especially of Ni (Fig. 7). According to qualitative EDX analyses, the protective scale—that is still <1 μm after 15,000 h—consists of Cr- and silicon-(Si) rich oxides (e.g., silica [SiO_2]), which are known as efficient barriers for the diffusion of both oxygen and metals at the temperature under consideration. Owing to the enrichment of Cr in the scale, the Cr content in a near-surface zone of the steel decreased, while a depletion of Si is less obvious from the qualitative EDX analyses applied. In general, the steel beneath the thin oxide layer is enriched in Ni, underlining the efficiency of the formed oxides with

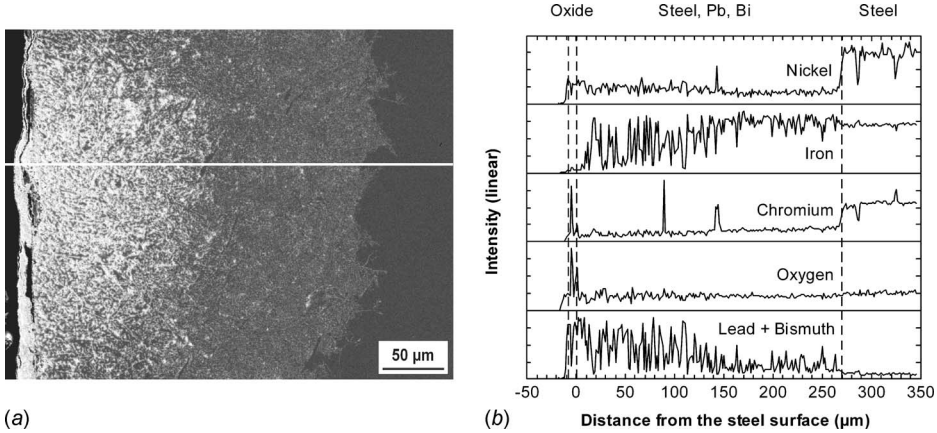

(*a*) (*b*)

Fig. 7 (*a*) Local degradation of 316L by selective leaching after exposure for 7518 h to flowing oxygen-containing LBE at 550°C (v=2 m/s; $c_O \approx 1.6\times10^{-6}$ mass %). (*b*) Results of qualitative EDX analyses along the line indicated in the electron-optical micrograph.

respect to the suppression of metal diffusion. Depletion of Ni underneath this scale was only once observed on a specimen that was exposed for 1991 h and might indicate incipient loss of the protective properties at the specific site investigated. The part of the total specimen surface protected by the thin oxide scale decreases with increasing exposure time and, after 15,000 h, is the exception rather than the rule.

The opposite extreme of corrosion behavior, i.e., selective leaching, is characterized by the removal of Ni, Cr, and potentially other (minor) alloying elements from a near-surface zone, followed by the penetration of Pb and Bi (Fig. 7). Where selective leaching did not proceed deep into the steel, depletion of Cr was less pronounced than indicated by the EDX linescan shown in Fig. 7. Owing to the significant depletion of Ni, the steel components not removed from the affected zone (essentially Fe) form a ferritic rather than an austenitic phase, which led to the use of "ferritization" as an alternative term for this corrosion phenomenon in the technical literature. Oxides found where severe selective leaching occurred are, in general, Cr-rich and form a thin scale on the surface of the depleted zone (Fig. 7) or a layer of irregular thickness (e.g., between 10 μm and 60 μm after exposure for 10,021 h) grown into the porous depleted steel. In the latter case, the porous zone was partly eroded by the liquid-metal flow. Alternatively, an almost hemispherical pit in the surface filled with Fe–Cr oxides was observed. However, only the thicker parts of the irregular Cr-rich oxide scale can account for the amount of Cr removed from the depleted zone, so that Cr transported in the liquid-metal phase penetrating the steel does not generally oxidize before reaching the steel surface, i.e., predominantly oxidizes after entering the LBE flow. In contrast to Ni—exhibiting a much higher solubility in LBE [4] and oxides of which were unstable for most of the exposure time (Fig. 1)—significant dissolution of Cr requires that oxygen is virtually completely removed from the liquid-metal phase, e.g., by oxidation of Fe and Cr, encountering the liquid metal when penetrating the steel. If, after advancing to a certain depth, the oxygen activity is sufficiently low for Cr dissolution, diffusion toward the steel surface enhances oxygen depletion of the succeeding liquid metal, so that retardation of selective leaching by oxidation of the steel at the penetration front is then impossible. Considering exposure experiments performed at temperatures between 420°C and 600°C under otherwise comparable conditions [10,11], selective leaching becomes important for the performance of austenitic steels in oxidizing LBE at temperatures around 550°C and is especially pronounced at 600°C.

Besides protective oxide scale formation and selective leaching—constituting the ideal and negative extrema of the behavior of 316L, respectively—the specimens showed enhanced oxidation that starts locally as indicated by the oxide-filled pits in the steel surface (Fig. 6(*b*)). With increasing exposure time, enhanced oxidation results in a partially continuous scale (Fig. 6(*c*)) observed in addition to isolated pits. The products of enhanced oxidation are Fe–Cr mixed oxides, most likely Cr-deficient spinel. Fe_3O_4 was occasionally found on top of the inward-growing mixed oxide but, in general, was missing. For exposure times $\leq$2000 h, Ni is uniformly distributed in the oxide-filled pits and, for $\geq$4000 h, largely confined to the bottom of the pits or the inner part of the continuous scale. In view of the conditions with respect to c_O (Fig. 1), Ni is dispersed in the mixed oxide in form of metallic particles rather than a component of the oxide. In some cases, the continuous scale partially consists of Cr-rich oxide in which metallic Pb and Bi are finely distributed, possibly indicating that this specific scale resulted from oxidation of the steel subsequent to selective leaching, which is corroborated by the occasional observation of the characteristic Ni-depletion and penetration of Pb and Bi in the steel beneath the scale.

Remeasuring the diameter of the 316L specimens after exposure to oxygen-containing flowing LBE showed that, except for the described local phenomena, the resulting material loss (metal recession) is in the order of the expected error of the metallographic method applied. For characterization of the material loss due to selective leaching after a specific exposure time, the maximum thickness of the depleted zone observed in the cross section of the respective specimens was measured using, if possible, the virtually noncorroded surrounding of the affected site as a reference. In general, only one or two sites exhibiting selective leaching were observed in the examined cross sections, with a considerable spread along the material surface amounting 2% and 8% of the specimen circumference after exposure for 1991 h and 10,021 h, respectively. In the latter case, a part of the (porous) depleted zone was eroded by the liquid-metal flow and had to be reconstructed in the micrograph. Selective leaching did not occur in the cross sections examined after exposure for 503 h, 1001 h, and 4015 h. The results of quantifying selective leaching are depicted in the top part of Fig. 8, showing a maximum material loss of 350 μm after 10,021 h. Additionally, the evolution of selective leaching based on a linear rate law is indicated, which, however, cannot account for the potentially different incubation times for this process at the evaluated sites. In the case of enhanced oxidation, the accompanying metal recession was also directly measured using the surface of the mixed oxide as a marker for the initial steel surface. For exposure times $\leq$2000 h, only a few spots in the examined cross sections were affected, from which the apparent maximum was selected. Especially after exposure for 7518 h and 15,028 h—when the percentage of enhanced oxidation was comparatively high and resulted in a partially continuous scale on the steel surface—the average from several measurements in different positions was determined. According to the results, which are summarized at the bottom part of Fig. 8, the maximum metal recession observed is in the range 30–50 μm after 7518 h. On average, the metal recession is approximately one order of magnitude lower than the material loss due to selective leaching and, therefore, less critical for the structural integrity of 316L. With respect to a detrimental effect on heat-transfer properties, locally enhanced oxidation might become significant after 7500–15,000 h.

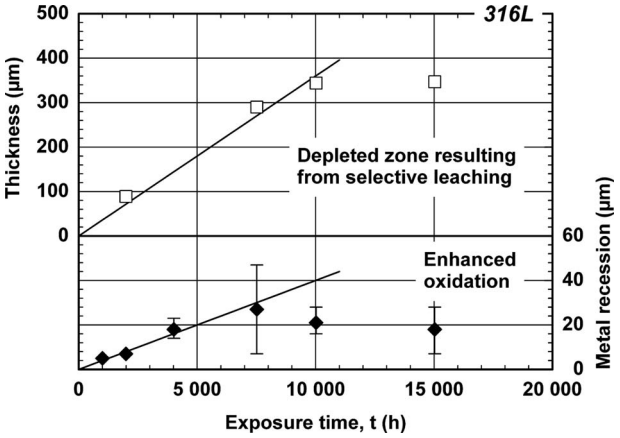

Fig. 8 Material loss due to local corrosion phenomena as a function of time for 316L after exposure to flowing oxygen-containing LBE at 550°C (v=2 m/s; $c_O \approx 1.6\times10^{-6}$ mass %). Top: (Maximum) thickness of the depleted zone resulting from selective leaching of Ni and Cr. Bottom: Metal recession accompanying enhanced oxidation.

An important point that did not become especially apparent from the results of the post-test examinations is the initiation of enhanced oxidation and the more critical selective leaching concurrently with the establishment of a Cr- and Si-rich protective oxide scale. Near-surface inclusions of manganese (Mn) sulfide or slag particles that were occasionally found in the microstructure of 316L impede protective scale formation and potentially cause local corrosion phenomena. Additionally, variously composed pre-

cipitates that formed in the course of the exposure at 550°C may influence the local performance of the steel. However, considering the small size of inclusions and precipitates found in comparison to the thickness of the oxides formed by enhanced oxidation or the depleted zone originating from selective leaching, it seems hardly possible to detect an effect on the initiation of these processes with the methods of analysis applied so far. Potential reasons for local breakdown of the protective scale independent of inclusions and precipitates in the steel microstructure are the very low but nonzero solubility of Cr-rich oxides in LBE—i.e., weakening of the protective scale by continuous dissolution and reprecipitation—and mechanical degradation by the liquid-metal flow. In general, protection by the thin oxide scale should be more persistent when the Si-rich component forms a continuous sublayer, which likely is the reason for the observed beneficial effect of Si on the performance of austenitic steels in LBE [12,13]. However, in view of detrimental effects on mechanical properties, appropriate amounts of Si added to these steels are generally limited [12].

4 Summary

Analyzing the performance of the F/M steel T91 and austenitic 316L in oxygen-containing flowing LBE at 550°C, $v=2$ m/s, and $c_O \approx 1.6\times10^{-6}$ mass % for exposure times up to 15,000 h showed that both steels are capable of forming oxide scales separating the steel from liquid metal. The oxide scale formed on T91 generally consists of a layer of Cr-deficient Fe–Cr spinel and an internal oxidation zone at the interface with the steel. Extrapolating the material loss (metal recession) determined by metallographic measurements to a service time of 100,000 h results in 50–70 μm, if a logarithmic or general power law is used to describe the evolution of the metal recession with time, and ~170 μm, if the parabolic trend in the data for exposure times ≤4000 h is considered (worst case). Setting a limit of 100 μm, the minimum service time is 4 years. The thickness of the spinel layer that potentially reduces the efficiency of heat-transfer surfaces is in the order of the metal recession, unless significant spalling occurs. Fe diffusing in the spinel layer is predominantly dissolved in the LBE (instead of forming Fe_3O_4 on top of the spinel), with fluxes <1 mg/m^2 h after 1000 h for logarithmic growth of the spinel layer and <10 mg/m^2 h after 1000 h if parabolic growth is assumed. Alternatively, an exceptionally thin scale consisting of Cr-rich oxide establishes on the surface of T91 but, in the long term, merges into the faster-growing scale. In the case of 316L, a thin protective scale consisting of Cr- and Si-rich oxides persists locally up to the longest exposure time investigated, with negligible material loss beneath this scale. Significant spinel formation occurs in connection with a locally starting enhanced oxidation process, replacing the thin scale with increasing exposure time. Enhanced oxidation of 316L may result in a local metal recession (and spinel thickness) in the range 30–50 μm after 7518 h, strongly depending on a variable incubation time for this locally starting process.

However, the liquid metal acts not only as a source of oxygen for oxidation processes and a sink for steel constituents not completely retained in the oxide scale originating on the surface but also participates actively in locally occurring degradation mechanisms. In the case of T91, liquid metal accumulates in the inner part of the spinel layer after entering the scale along cracks and possibly also via open porosity. An especially crucial situation arises, if, possibly starting from a certain amount of oxygen-depleted liquid metal at the scale/steel interface, Cr is selectively dissolved from the steel, accompanied by penetration of Pb and Bi into the Cr-depleted steel matrix and a comparatively high local material degradation. For 316L, selective leaching is especially pronounced, as Ni—exhibiting a high solubility in LBE and a negligible driving-force for oxidation under the experimental conditions—dissolves first, opening paths for the penetration of Pb and Bi into the steel. With increasing penetration depth, i.e., oxygen-depletion in the liquid metal, Cr also dissolves significantly, reducing the probability of a retardation of selective leaching by oxidation at the penetration front. The maximum local damage observed on specimens of T91 and 316L is 150–170 μm after 15,028 h and 350 μm after 10,021 h, respectively. For long-term use in LBE, selective leaching has to be prevented, e.g., by optimizing Cr supply to the surface or, in the case of 316L, a moderately higher Si content.

Acknowledgment

The presented study was funded by the EURATOM Sixth Framework Programme as part of the IP EUROTRANS (Contract No. FI6W-CT-2004-516520). Special thanks go to O. Wedemeyer, Z. Voss, J. Novotny, and A. Skrypnik for preparing the exposure experiments and operating the CORRIDA loop.

Nomenclature

c_O	=	oxygen concentration
E	=	output of oxygen sensors
j_{Fe}	=	iron flux
K	=	degree Kelvin
T	=	temperature
t	=	time
V	=	volts
v	=	flow velocity
Δx	=	metal recession
Δx_{sp}, Δx_{IOZ}	=	thickness of spinel layer and IOZ, respectively
$\Delta\rho_{Fe}$	=	change in iron partial density

References

[1] Van den Bosch, J., and Almazouzi, A., 2005, "Procurement and Characterisation of T91 and SS316L Plates," SCK-CEN Report No. SCK-CEN-R-4197.

[2] Schroer, C., Voss, Z., Novotny, J., and Konys, J., 2006, "Quantification of the Degradation of Steels Exposed to Liquid Lead-Bismuth Eutectic," Forschungszentrum Karlsruhe Report No. FZKA 7224 (http://bibliothek.fzk.de/zb/berichte/FZKA7224.pdf).

[3] Schroer, C., Voss, Z., Wedemeyer, O., Novotny, J., and Konys, J., 2006, "Oxidation of Steel T91 in Flowing Lead-Bismuth Eutectic (LBE) at 550°C," J. Nucl. Mater., **356**(1–3), pp. 189–197.

[4] Schroer, C., and Konys, J., 2007, "Physical Chemistry of Corrosion and Oxygen Control in Liquid Lead and Lead-Bismuth Eutectic," Forschungszentrum Karlsruhe Report No. FZKA 7364 (http://bibliothek.fzk.de/zb/berichte/FZKA7364.pdf).

[5] Martinelli, L., Balbaud-Célérier, F., Terlain, A., Delpech, S., Santarini, G., Favergeon, J., Moulin, G., Tabarant, M., and Picard, G., 2008, "Oxidation Mechanism of a Fe-9Cr-1Mo Steel by Liquid Pb-Bi Eutectic Alloy (Part I)," Corros. Sci., **50**(9), pp. 2523–2536.

[6] Mueller, G., Schumacher, G., and Zimmermann, F., 2000, "Investigation of Oxygen Controlled Liquid Lead Corrosion of Surface Treated Steels," J. Nucl. Mater., **278**(1), pp. 85–95.

[7] Martinelli, L., Balbaud-Célérier, F., Terlain, A., Bosonnet, S., Picard, G., and Santarini, G., 2008, "Oxidation Mechanism of a Fe-9Cr-1Mo Steel by Liquid Pb-Bi Eutectic Alloy (Part I)," Corros. Sci., **50**(9), pp. 2537–2548.

[8] Weisenburger, A., Heinzel, A., Mueller, G., Muscher, H., and Rousanov, A., 2008, "T91 Cladding Tubes With and Without Modified FeCrAlY Coatings Exposed in LBE at Different Flow, Stress and Temperature Conditions," J. Nucl. Mater., **376**(3), pp. 274–281.

[9] Schroer, C., Konys, J., Furukawa, T., and Aoto, K., 2010, "Oxidation Behaviour of P122 and a 9Cr-2W ODS Steel at 550°C in Oxygen-Containing Flowing Lead-Bismuth Eutectic," J. Nucl. Mater., **398**(1-3), pp. 109–115.

[10] Mueller, G., Heinzel, A., Konys, J., Schumacher, G., Weisenburger, A., Zimmermann, F., Engelko, V., Rusanov, A., and Markov, V., 2002, "Results of Steel Corrosion Tests in Flowing Liquid Pb/Bi at 420–600°C After 2000 h," J. Nucl. Mater., **301**(1), pp. 40–46.

[11] Mueller, G., Heinzel, A., Konys, J., Schumacher, G., Weisenburger, A., Zimmermann, F., Engelko, V., Rusanov, A., and Markov, V., 2002, "Behavior of Steels in Flowing Liquid PbBi Eutectic Alloy at 420–600°C After 4000–7200 h," J. Nucl. Mater., **335**(2), pp. 163–168.

[12] Gorynin, I. V., Karzov, G. P., Markov, V. G., and Yakolev, V. A., 1999, "Structural Materials for Atomic Reactors With Liquid Metal Heat-Transfer Agents in the Form of Lead and Lead-Bismuth Alloy," Metal Sci. Heat Treat., **41**(9–10), pp. 384–388.

[13] Kurata, Y., Futakawa, M., and Saito, S., 2008, "Corrosion Behavior of Steels in Liquid Lead-Bismuth With Low Oxygen Concentrations," J. Nucl. Mater., **373**(1-3), pp. 164–178.